

Electronic Supplementary Information for

**The synthesis of iron-doped 3D ordered mesoporous cobalt  
phosphide material to towards Efficient Electrochemical Overall  
Water Splitting**

Suci Meng,<sup>a</sup> Shichao Sun,<sup>a</sup> Yue Qi,<sup>a</sup> Deli Jiang,<sup>\*a</sup> Wenxian Wei<sup>b</sup> and Min Chen<sup>\*a</sup>

<sup>a</sup> School of Chemistry and Chemical Engineering, Jiangsu University, 301 Xuefu  
Road, Zhenjiang 212013, China

<sup>b</sup> Testing Center, Yangzhou University, 48 East Wenhui Road, Yangzhou 225009,  
China

Corresponding author: Min Chen, Deli Jiang

E-mail address: chenmin3226@sina.com, dlj@ujs.edu.cn

# Contents

<b>Fig. S1</b> SEM image of the as-synthesized SBA-15.	1
<b>Fig. S2</b> TEM image of the as-synthesized SBA-15.	2
<b>Fig. S3</b> SEM image of the as-synthesized Meso-Co <sub>2</sub> P.	3
<b>Fig. S4</b> TEM image of the as-synthesized Meso-CoP.	4
<b>Fig. S5</b> SEM image of the as-synthesized Meso-Co <sub>3</sub> O <sub>4</sub> .	5
<b>Fig. S6</b> SEM image of the as-synthesized Bulk-Co <sub>2</sub> P.	6
<b>Fig. S7</b> SEM image of the as-synthesized Bulk-Co <sub>1.8</sub> Fe <sub>0.2</sub> P.	7
<b>Fig. S8</b> LSV and Tafel plots of different iron additions for the HER.	8
<b>Fig. S9</b> CV curves of Meso-Co <sub>1.8</sub> Fe <sub>0.2</sub> P for HER and OER.	9
<b>Fig. S10</b> LSV and Tafel plots of different iron additions for the OER.	10
<b>Table S1.</b> Elemental composition (atomic and weight percentage) obtained from ICP analysis.	11
<b>Table S2.</b> The simulated series resistance (R <sub>s</sub> ) and charge transfer resistance (R <sub>ct</sub> ).	12
<b>Table S3.</b> Comparison table with other reported HER catalysts.	13
<b>Table S4.</b> Comparison table with other reported OER catalysts.	14
<b>Table S5.</b> Comparison table with other reported bifunctional catalysts.	15
<b>References</b>	16

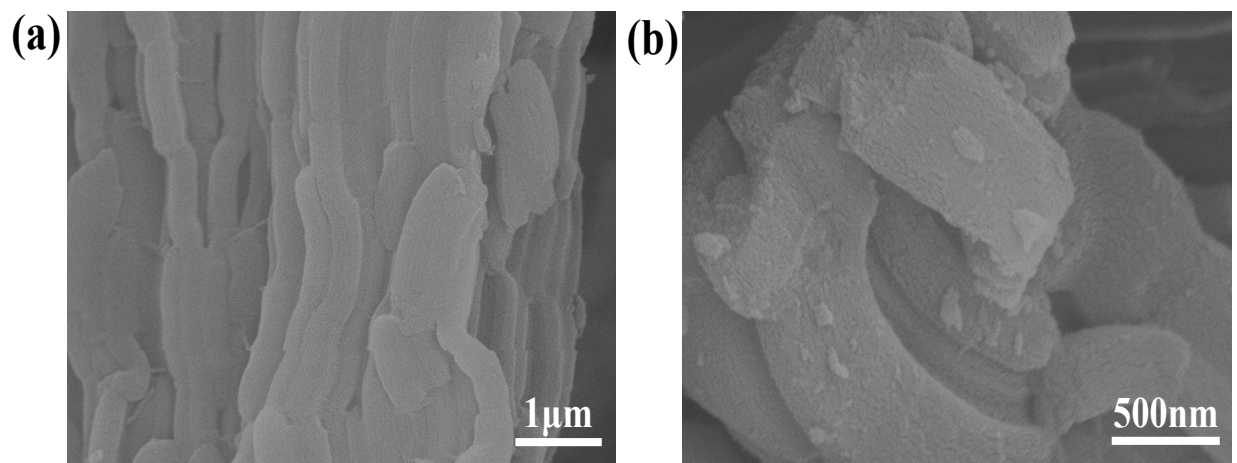


**Fig. S1** SEM image of the as-synthesized SBA-15.

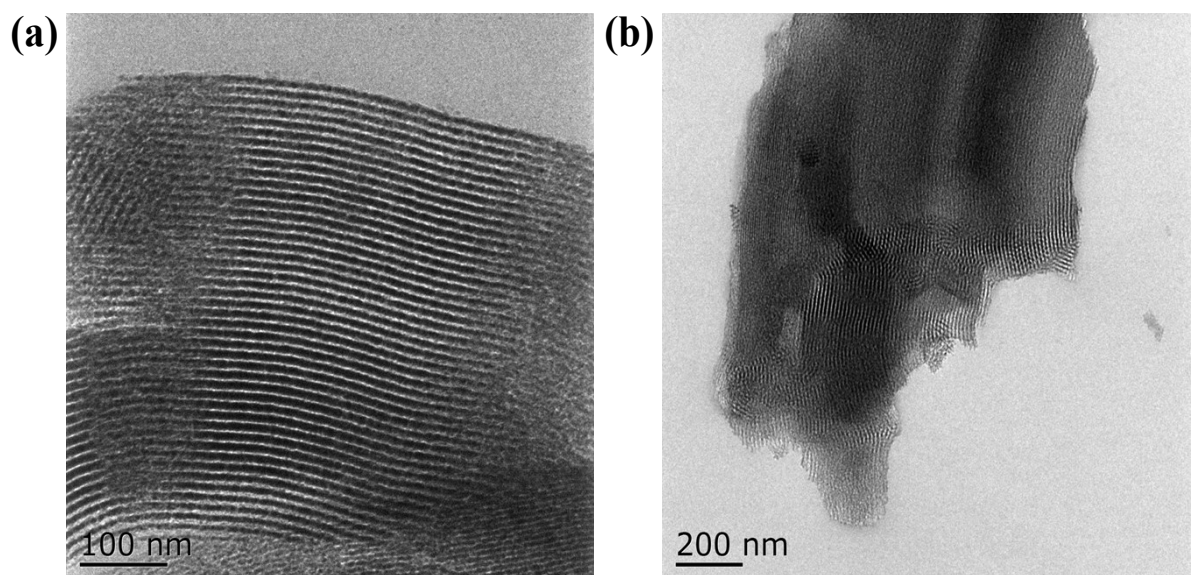


**Fig. S2** TEM image of the as-synthesized SBA-15.

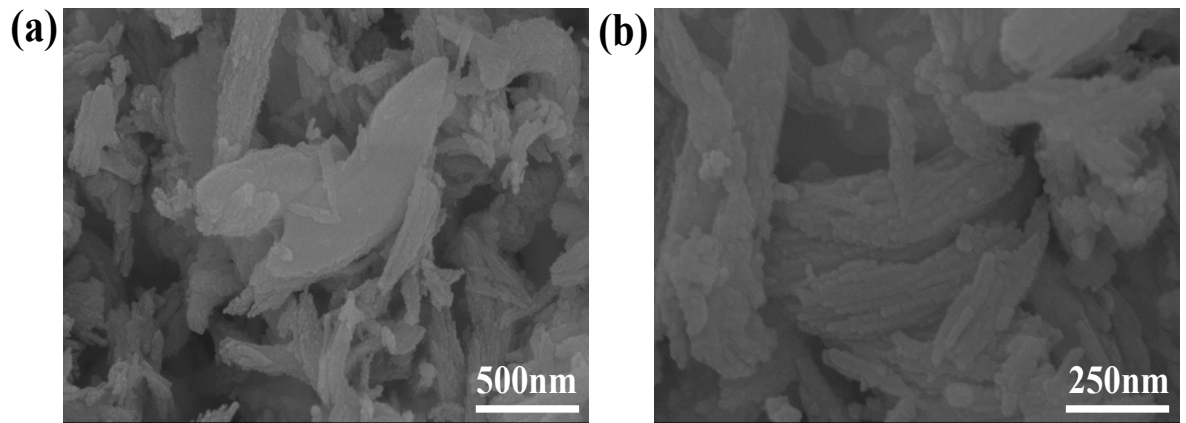


**Fig. S3** SEM image of the as-synthesized Meso-CoP.

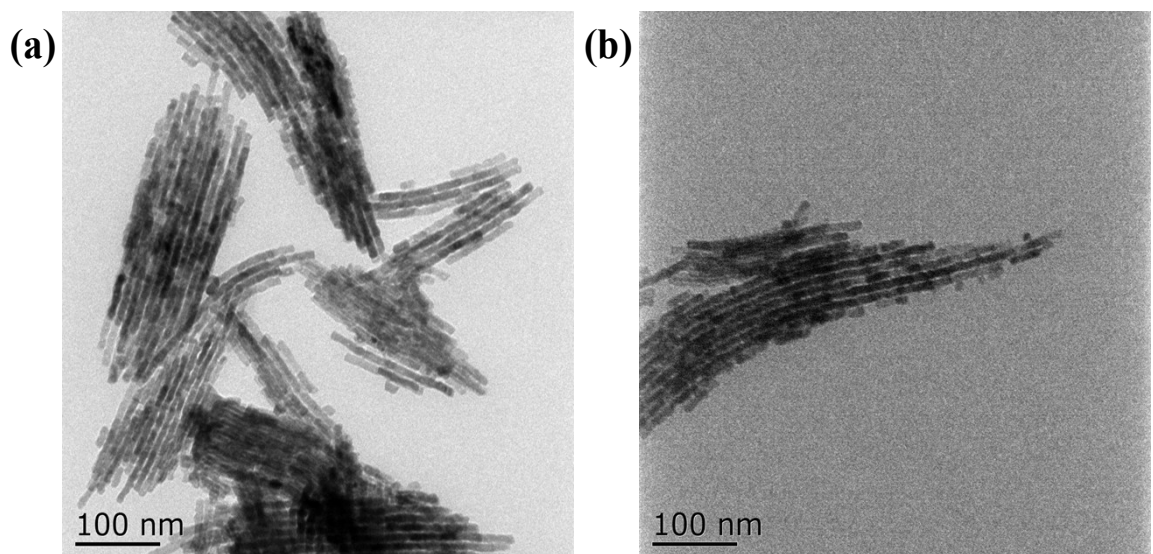


**Fig. S4** TEM image of the as-synthesized Meso-Co<sub>2</sub>P.

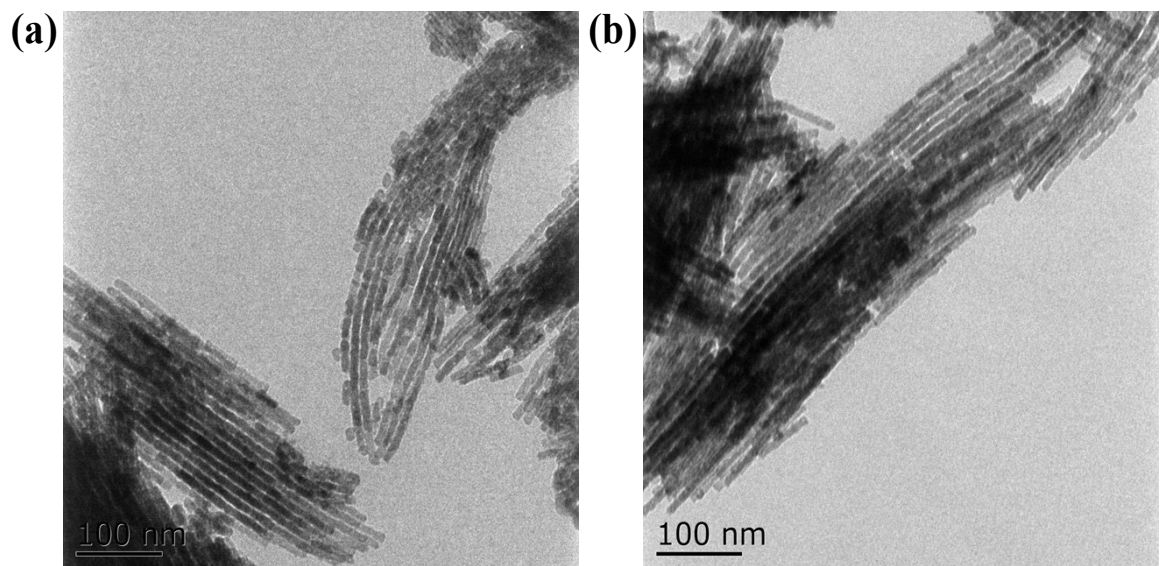


**Fig. S5** SEM image of the as-synthesized Meso-Co<sub>3</sub>O<sub>4</sub>.

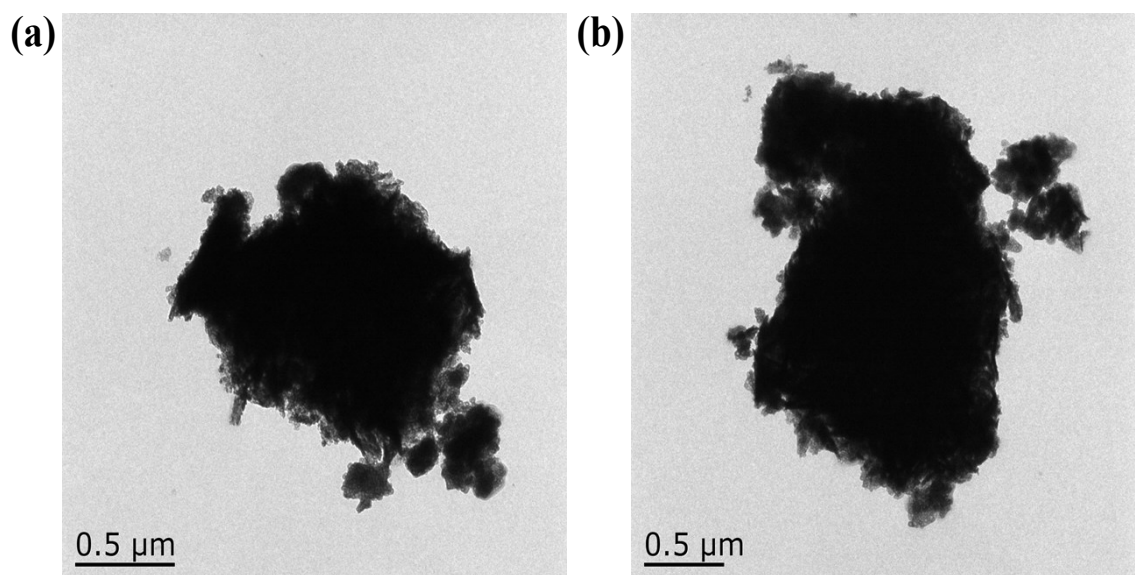


**Fig. S6** SEM image of the as-synthesized Bulk-Co<sub>2</sub>P.

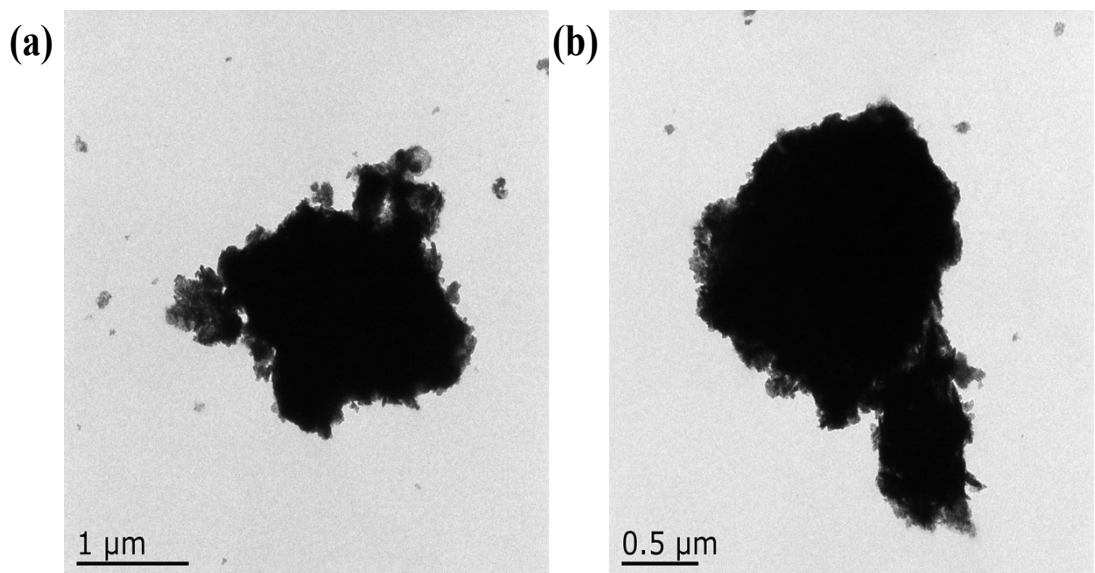


**Fig. S7** SEM image of the as-synthesized Bulk-Co<sub>1.8</sub>Fe<sub>0.2</sub>P.

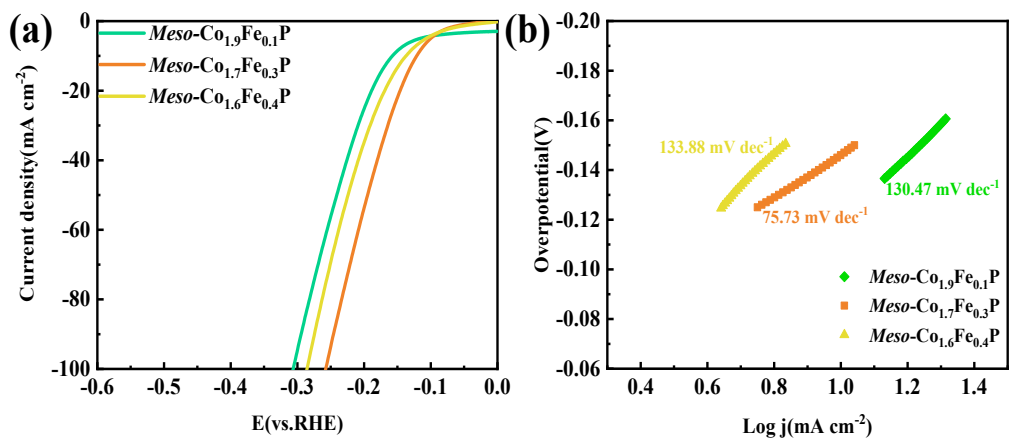


**Fig. S8** (a) Linear sweep polarization curves of different iron additions for the HER at a scan rate of 2 mV s<sup>-1</sup> in 1 M KOH solution; (b) Tafel plots.

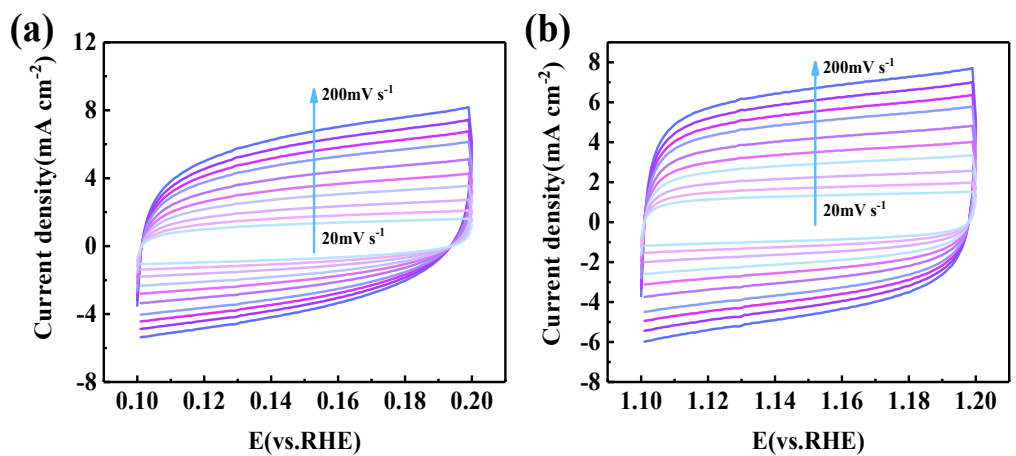


**Fig. S9** CV curves measured of Meso-Co<sub>1.8</sub>Fe<sub>0.2</sub>P in 1 M KOH at the scan rates from 20 to 200  $\text{mV s}^{-1}$  for (a) HER, (b) OER.

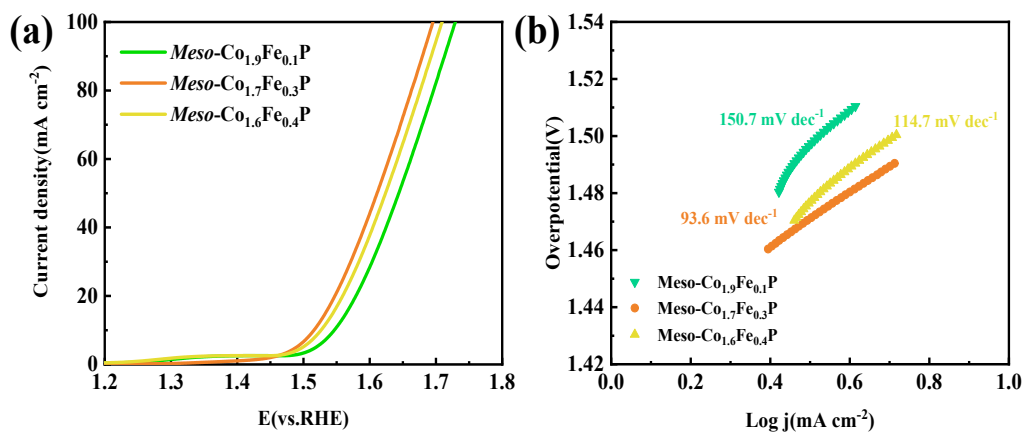


**Fig. S10** (a) Linear sweep polarization curves of different iron additions for the HER at a scan rate of 2 mV s<sup>-1</sup> in 1 M KOH solution; (b) Tafel plots.

**Table S1.** Elemental composition (atomic and weight percentage) obtained from ICP analysis.

Electrocatalysts	Weight % (Co, Fe)	Co/Fe (Atom ratio)
<b>Meso-Co<sub>1.9</sub>Fe<sub>0.1</sub>P</b>	<b>10.247</b>	<b>0.507</b>
<b>Meso-Co<sub>1.8</sub>Fe<sub>0.2</sub>P</b>	<b>11.886</b>	<b>1.261</b>
<b>Meso-Co<sub>1.6</sub>Fe<sub>0.4</sub>P</b>	<b>10.845</b>	<b>2.526</b>

**Table S2.** The simulated series resistance ( $R_s$ ) and charge transfer resistance ( $R_{ct}$ ) in the presence of as-prepared electrodes.

Sample	Reaction	$R_{ct} (\Omega)$	$R_s (\Omega)$
<b>Meso-Co<sub>1.8</sub>Fe<sub>0.2</sub>P</b>	HER	42.7	20.29
	OER	17.6	10.13
<b>Meso-Co<sub>2</sub>P</b>	HER	83.4	21.21
	OER	58.2	10.29
<b>Bulk-Co<sub>1.8</sub>Fe<sub>0.2</sub>P</b>	HER	110.7	20.15
	OER	90.5	10.46
<b>Bulk-Co<sub>2</sub>P</b>	HER	166.1	21.10
	OER	153.6	10.92

**Table S3.** Comparison of the catalytic activity toward the HER in 1 M KOH of the Meso-Co<sub>1.8</sub>Fe<sub>0.2</sub>P with other reported high performance HER catalysts.

Catalyst	$\eta$ (mV) at $J = 10 \text{ mA cm}^{-2}$	Tafel slope (mV dec <sup>-1</sup> )	Reference
<b>Meso-Co<sub>1.8</sub>Fe<sub>0.2</sub>P</b>	93.7	84.5	This Work
<b>o-CoSe<sub>2</sub> P</b>	104	96	[1]
<b>(Co<sub>1-x</sub>Ni<sub>x</sub>)(S<sub>1-y</sub>P<sub>y</sub>)<sub>2</sub>/G</b>	117	85	[2]
<b>f-CoP/CoP<sub>2</sub>/Al<sub>2</sub>O<sub>3</sub></b>	138	76	[3]
<b>CoP<sub>3</sub>/Ni<sub>2</sub>P</b>	115	49	[4]
<b>Ni-CoP/HPFs</b>	92	52	[5]
<b>CoP<sub>x</sub>/N-rGO</b>	104	65	[6]
<b>CoFe–Se–P</b>	172.5	58	[7]
<b>o-Co<sub>2</sub>P</b>	160	60.1	[8]
<b>Ni-Co-P</b>	150	60.6	[9]
<b>Co(S<sub>0.71</sub>Se<sub>0.29</sub>)<sub>2</sub></b>	145	80.7	[10]
<b>EG/H-Co<sub>0.86</sub>Se P</b>	170	86	[11]
<b>CoP@a-CoO<sub>x</sub></b>	132	89	[12]
<b>N-doped CoP<sub>2</sub>/CC</b>	64	47.4	[13]
<b>NiP/CFP</b>	100	85.4	[14]
<b>Ni<sub>2</sub>P/NF</b>	150	86	[15]

**Table S4.** Comparison of the catalytic activity toward the OER in 1 M KOH of the Meso-Co<sub>1.8</sub>Fe<sub>0.2</sub>P with other reported high performance OER catalysts.

Catalyst	$\eta$ (mV) at $J = 10 \text{ mA cm}^{-2}$	Tafel slope	Reference
		(mV dec <sup>-1</sup> )	
<b>Meso-Co<sub>1.8</sub>Fe<sub>0.2</sub>P</b>	266.4	80.6	This Work
(Co <sub>1-x</sub> Ni <sub>x</sub> )(S <sub>1-y</sub> P <sub>y</sub> ) <sub>2</sub> /G	285	105	[2]
<b>f-CoP/CoP<sub>2</sub>/Al<sub>2</sub>O<sub>3</sub></b>	300	63	[3]
<b>CoFe–Se–P</b>	230	108	[7]
<b>CoP@a-CoO<sub>x</sub></b>	232	89	[12]
<b>Co/Co<sub>x</sub>M<sub>y</sub></b>	334	79.2	[16]
<b>Co<sub>3</sub>O<sub>4</sub>@BP</b>	400	63	[17]
<b>Fe–CoS<sub>2</sub></b>	302	85	[18]
<b>CeO<sub>x</sub>/CoS@S–CeO<sub>2</sub></b>	269	50	[19]
<b>Fe/Co (1.3:100)</b>	322	N/A	[20]
<b>P-Co<sub>3</sub>O<sub>4</sub></b>	280	51.6	[21]
<b>(Co<sub>4</sub>Mn<sub>1</sub>)Se<sub>2</sub></b>	274	39	[22]
<b>CMP@PNC</b>	~330	88	[23]
<b>N-C-CoFe</b>	290	100	[24]
<b>CoPPi</b>	359	54.1	[25]
<b>CoNi<sub>0.2</sub>Fe<sub>0.05</sub>-Z-H-P</b>	329	48	[26]

**Table S5.** Comparison of the catalytic activity toward the overall water splitting in 1 M KOH of the Meso-Co<sub>1.8</sub>Fe<sub>0.2</sub>P with other reported high performance bifunctional catalysts.

Catalyst	Cell voltages (V) at $J = 10\text{mA cm}^{-2}$	Reference
<b>Meso-Co<sub>1.8</sub>Fe<sub>0.2</sub>P   Meso-Co<sub>1.8</sub>Fe<sub>0.2</sub>P</b>	1.58	This Work
(Co <sub>1-x</sub> Ni <sub>x</sub> )(S <sub>1-y</sub> P <sub>y</sub> ) <sub>2</sub> /G   (Co <sub>1-x</sub> Ni <sub>x</sub> )(S <sub>1-y</sub> P <sub>y</sub> ) <sub>2</sub> /G	1.65	[2]
f-CoP/CoP <sub>2</sub> /Al <sub>2</sub> O <sub>3</sub>    f-CoP/CoP <sub>2</sub> /Al <sub>2</sub> O <sub>3</sub>	1.65	[3]
CoFe–Se–P   CoFe–Se–P	1.59	[7]
CoP@a-CoO <sub>x</sub>    CoP@a-CoO <sub>x</sub>	1.66	[12]
CMS-16h   CMS-16h	1.71	[27]
np-Co <sub>9</sub> S <sub>4</sub> P <sub>4</sub>    np-Co <sub>9</sub> S <sub>4</sub> P <sub>4</sub>	1.67	[28]
CoP/Co <sub>9</sub> S <sub>8</sub>    CoP/Co <sub>9</sub> S <sub>8</sub>	1.6	[29]
CoPS/Al <sub>2</sub> O <sub>3</sub> -3   CoPS/Al <sub>2</sub> O <sub>3</sub> -3	1.75	[30]
Co <sub>2</sub> B/CoSe <sub>2</sub>    Co <sub>2</sub> B/CoSe <sub>2</sub>	1.73	[31]
Co <sub>1-x</sub> Fex-LDH(+)   Ni <sub>1-x</sub> Fex-LDH(-)	1.59	[32]
MoS <sub>2</sub> /NPF CoFe <sub>2</sub> O <sub>4</sub>    MoS <sub>2</sub> /NPF CoFe <sub>2</sub> O <sub>4</sub>	1.58	[33]
CoP/NCNHP   CoP/NCNHP	1.64	[34]
NiCoSe <sub>2</sub>    NiCoSe <sub>2</sub>	1.62	[35]
P-Co <sub>3</sub> O <sub>4</sub> /NF   P-Co <sub>3</sub> O <sub>4</sub> /NF	1.63	[36]
Co <sub>0.75</sub> Ni <sub>0.25</sub> Se/NF  Co <sub>0.75</sub> Ni <sub>0.25</sub> Se/NF	1.61	[37]

## References

1. Y. R. Zheng, P. Wu, M. R. Gao, X. L. Zhang, F. Y. Gao, H. X. Ju, R. Wu, Q. Gao, R. You, W. X. Huang, S. J. Liu, S. W. Hu, J. F. Zhu, Z. Y. Li, S. H. Yu, Doping-induced structural phase transition in cobalt diselenide enables enhanced hydrogen evolution catalysis, *Nat. Commun.*, 2018, **9**, 2533. DOI: 10.1038/s41467-018-04954-7.
2. H. J. Song, H. Yoon, B. Ju, G. H. Lee, D. W. Kim, 3D Architectures of quaternary Co-Ni-S-P/graphene hybrids as highly active and stable bifunctional electrocatalysts for overall water splitting, *Adv. Energy Mater.*, 2018, **8**, 1802319. DOI: 10.1002/aenm.201802319.
3. W. Li, S. Zhang, Q. Fan, F. Zhang, S. Xu, Hierarchically scaffolded CoP/CoP<sub>2</sub> nanoparticles: controllable synthesis and their application as a well-matched bifunctional electrocatalyst for overall water splitting, *NanoScale*, 2017, **9**, 5677–5685. DOI: 10.1039/C7NR01017F.
4. K. Wang, X. She, S. Chen, H. Liu, D. Li, Y. Wang, H. Zhang, D. Yang, X. Yao, Boosting hydrogen evolution via optimized hydrogen adsorption at the interface of CoP<sub>3</sub> and Ni<sub>2</sub>P, *J. Mater. Chem. A*, 2018, **6**, 5560–5565. DOI: 10.1039/C7TA10902D.
5. Y. Pan, K. Sun, Y. Lin, X. Cao, Y. Cheng, S. Liu, L. Zeng, W. C. Cheng, D. Zhao, K. Wu, Electronic structure and d-band center control engineering over M-doped CoP (M=Ni, Mn, Fe) hollow polyhedron frames for boosting hydrogen production, *Nano Energy*, 2019, **56**, 411–419. DOI: 10.1016/j.nanoen.2018.11.034.
6. L. Zheng, W. Hu, X. Shu, H. Zheng, X. Fang, Ultrafine CoP<sub>x</sub> nanoparticles anchored on nitrogen doped reduced graphene oxides for superior hydrogenation in alkaline media, *Adv. Mater. Interfaces.*, 2018, **5**, 1800515. DOI: 10.1002/admi.201800515.
7. L. He, B. Cui, B. Hu, J. Liu, K. Tian, M. Wang, Y. Song, S. Fang, Z. Zhang, Q. Jia, Mesoporous

- nanostructured CoFe–Se–P composite derived from a prussian blue analogue as a superior electrocatalyst for efficient overall water splitting, *ACS Appl. Mater. Interfaces*, 2018, **1**, 3915–3928. DOI: 10.1021/acsami.8b00663.
8. K. Xu, H. Ding, M. Zhang, M. Chen, Z. Hao, L. Zhang, C. Wu, Y. Xie, Regulating water-reduction kinetics in cobalt phosphide for enhancing her catalytic activity in alkaline solution, *Adv. Mater.*, 2017, **29**, 1606980. DOI: 10.1002/adma.201606980.
9. Y. Feng, X.-Y. Yu, U. Paik, Nickel cobalt phosphides quasi-hollow nanocubes as an efficient electrocatalyst for hydrogen evolution in alkaline solution, *Chem. Commun.*, 2016, **52**, 1633–1636. DOI: 10.1039/C5CC08991C.
10. L. Fang, W. Li, Y. Guan, Y. Feng, H. Zhang, S. Wang, Y. Wang, Tuning unique peapod-like  $\text{Co}(\text{S}_x\text{Se}_{1-x})_2$  nanoparticles for efficient overall water splitting, *Adv. Funct. Mater.*, 2017, **27**, 1701008. DOI: 10.1002/adfm.201701008.
11. Y. Hou, M. Qiu, T. Zhang, X. Zhuang, C. S. Kim, C. Yuan, X. Feng, Ternary porous cobalt phosphoselenide nanosheets: an efficient electrocatalyst for electrocatalytic and photoelectrochemical water splitting, *Adv. Mater.*, 2017, **29**, 1701589. DOI: 10.1002/adma.201701589.
12. J. Yu, Y. Zhong, X. Wu, J. Sunarso, M. Ni, W. Zhou, Z. Shao, Bifunctionality from synergy: CoP nanoparticles embedded in amorphous  $\text{CoO}_x$  nanoplates with heterostructures for highly efficient water electrolysis, *Adv. Sci.*, 2018, **5**, 1800514. DOI: 10.1002/advs.201800514.
13. L. Wang, H. Wu, S. Xi, S. T. Chua, F. Wang, S. J. Pennycook, Z. G. Yu, Y. Du, J. Xue, Nitrogen-doped cobalt phosphide for enhanced hydrogen evolution activity, *ACS Appl. Mater. Interfaces*, 2019, **11**, 17359–17367. DOI: 10.1021/acsami.9b01235.
14. X. Wang, L. Wei, D. Xiong, D. Y. Petrovykh, L. Liu, Bifunctional nickel phosphide nanocatalysts supported

- on carbon fiber paper for highly efficient and stable overall water splitting, *Adv. Funct. Mater.*, 2016, **26**, 4066–4066. DOI: 10.1002/adfm.201505509.
15. B. You, N. Jiang, X. Liu, Y. Sun, Simultaneous H<sub>2</sub> generation and biomass upgrading in water by an efficient noble-metal-free bifunctional electrocatalyst, *Angew. Chem. Int. Ed.*, 2016, **55**, 9913–9917. DOI: 10.1002/anie.201603798.
16. J. Chen, C. Fan, X. Hu, C. Wang, Z. Huang, G. Fu, J. M. Lee, Y. Tang, Hierarchically Porous Co/Co<sub>x</sub>M<sub>y</sub> (M=P, N) as an efficient mott-schottky electrocatalyst for oxygen evolution in rechargeable Zn-air batteries, *Small*, 2019, **15**, 1901518. DOI: 10.1002/smll.201901518.
17. F. Shi, K. Huang, Y. Wang, W. Zhang, L. Li, X. Wang, S. Feng, Black phosphorus modified Co<sub>3</sub>O<sub>4</sub> through tuning electronic structure for enhanced oxygen evolution reaction, *ACS Appl. Mater. Interfaces*, 2019, **11**, 17459–17466. DOI: 10.1021/acsami.9b04078.
18. W. Kong, X. Luan, H. Du, L. Xia, F. Qu, Enhanced electrocatalytic activity of water oxidation in an alkaline medium via Fe doping in CoS<sub>2</sub> nanosheets, *Chem. Commun.*, 2019, **55**, 2469–2472. DOI: 10.1039/C8CC10203A.
19. H. Xu, Y. Yang, X. Yang, J. Cao, W. Liu, Y. Tang, Stringing MOF-derived nanocages: a strategy for the enhanced oxygen evolution reaction, *J. Mater. Chem. A*, 2019, **7**, 8284–8291. DOI: 10.1039/C9TA00624A.
20. G. h. Moon, M. Yu, C. K. Chan, H. Tüysüz, Highly active cobalt-based electrocatalysts with facile incorporation of dopants for the oxygen evolution reaction, *Angew. Chem.*, 2019, **131**, 3529–3533. DOI: 10.1002/anie.201813052.
21. Z. Xiao, Y. Wang, Y. C. Huang, Z. Wei, C. L. Dong, J. Ma, S. Shen, Y. Li, S. Wang, Filling the oxygen vacancies in Co<sub>3</sub>O<sub>4</sub> with phosphorus: an ultra-efficient electrocatalyst for overall water splitting, *Energy Environ. Sci.*, 2017, **10**, 2563–2569. DOI: 10.1039/C7EE01917C.

22. X. Zhao, X. Li, Y. Yan, Y. Xing, S. Lu, L. Zhao, S. Zhou, Z. Peng, J. Zeng, Electrical and structural engineering of cobalt selenide nanosheets by Mn modulation for efficient oxygen evolution, *Appl. Catal., B*, 2018, **236**, 569–575. DOI: 10.1016/j.apcatb.2018.05.054.
23. S. Yang, Q. He, C. Wang, H. Jiang, C. Wu, Y. Zhang, T. Zhou, Y. Zhou, L. Song, Confined bimetallic phosphide within P, N co-doped carbon layers towards boosted bifunctional oxygen catalysis, *J. Mater. Chem. A*, 2018, **6**, 11281–11287. DOI: 10.1039/C8TA02897D.
24. A. Samanta, C. R. Raj, Catalyst support in oxygen electrocatalysis: a case study with CoFe alloy electrocatalyst, *The Journal of Physical Chemistry C*, 2018, **122**, 15843–15852. DOI: 10.1021/acs.jpcc.8b02830.
25. H. Du, W. Ai, Z. L. Zhao, Y. Chen, X. Xu, C. Zou, L. Wu, L. Su, K. Nan, T. Yu, Engineering morphologies of cobalt pyrophosphates nanostructures toward greatly enhanced electrocatalytic performance of oxygen evolution reaction, *Small*, 2018, **14**, 1801068. DOI: 10.1002/smll.201801068
26. M. Wang, C. L. Dong, Y. C. Huang, Y. Li, S. Shen, Electronic structure evolution in tricomponent metal phosphides with reduced activation energy for efficient electrocatalytic oxygen evolution, *Small*, 2018, **14**, 1801756. DOI: 10.1002/smll.201801756.
27. S. Shit, W. Jang, S. Bolar, N. C. Murmu, H. Koo, T. Kuila, Effect of ion diffusion in cobalt molybdenum bimetallic sulfide towards electrocatalytic water splitting, *ACS Appl. Mater. Interfaces*, 2019, **11**, 21634–21644. DOI: 10.1021/acsami.9b06635.
28. Y. Tan, M. Luo, P. Liu, C. Cheng, J. Han, K. Watanabe, M. Chen, Three-dimensional nanoporous Co<sub>9</sub>S<sub>4</sub>P<sub>4</sub> pentlandite as a bifunctional electrocatalyst for overall neutral water splitting, *ACS Appl. Mater. Interfaces*, 2019, **11**, 3880–3888. DOI: 10.1021/acsami.8b17961.
29. T. Meng, J. Qin, D. Xu, M. Cao, Atomic heterointerface-induced local charge distribution and enhanced

- water adsorption behavior in a cobalt phosphide electrocatalyst for self-powered highly efficient overall water splitting, *ACS Appl. Mater. Interfaces*, 2019, **11**, 9023–9032. DOI:10.1021/acsami.8b19341.
30. T. Wang, Y. Zhang, Y. Wang, J. Zhou, L. Wu, Y. Sun, X. Xu, W. Hou, X. Zhou, Y. Du, Alumina-supported CoPS nanostructures derived from LDH as highly active bifunctional catalysts for overall water splitting, *ACS Sustainable Chem. Eng.*, 2018, **6**, 10087–10096. DOI: 10.1021/acssuschemeng.8b01425.
31. Y. Guo, Z. Yao, C. Shang, E. Wang, Amorphous Co<sub>2</sub>B grown on CoSe<sub>2</sub> nanosheets as a hybrid catalyst for efficient overall water splitting in alkaline medium, *ACS Appl. Mater. Interfaces*, 2017, **9**, 39312–39317. DOI: 10.1021/acsami.7b10605.
32. G. Rajeshkhanna, T. I. Singh, N. H. Kim, J. H. Lee, Remarkable bifunctional oxygen and hydrogen evolution electrocatalytic activities with trace-level Fe doping in Ni-and Co-layered double hydroxides for overall water-splitting, *ACS Appl. Mater. Interfaces*, 2018, **10**, 42453–42468. DOI: 10.1021/acsami.8b16425.
33. J. Sun, N. Guo, Z. Shao, K. Huang, Y. Li, F. He, Q. Wang, A facile strategy to construct amorphous spinel-based electrocatalysts with massive oxygen vacancies using ionic liquid dopant, *Adv. Energy Mater.*, 2018, **8**, 1800980. DOI: 10.1002/aenm.201800980.
34. Y. Pan, K. Sun, S. Liu, X. Cao, K. Wu, W.-C. Cheong, Z. Chen, Y. Wang, Y. Li, Y. Liu, Core–shell ZIF-8@ZIF-67-derived CoP nanoparticle-embedded N-doped carbon nanotube hollow polyhedron for efficient overall water splitting, *J. Am. Chem. Soc.*, 2018, **140**, 2610–2618. DOI: 10.1021/jacs.7b12420.
35. J. Yu, Y. Tian, F. Zhou, M. Zhang, R. Chen, Q. Liu, J. Liu, C. Y. Xu, J. Wang, Metallic and superhydrophilic nickel cobalt diselenide nanosheets electrodeposited on carbon cloth as a bifunctional electrocatalyst, *J. Mater. Chem. A*, 2018, **6**, 17353–17360. DOI: 10.1039/C8TA04950E.
36. Z. Wang, H. Liu, R. Ge, X. Ren, J. Ren, D. Yang, L. Zhang, X. Sun, Phosphorus-doped Co<sub>3</sub>O<sub>4</sub> nanowire array: a highly efficient bifunctional electrocatalyst for overall water splitting, *ACS Catal.*, 2018, **8**, 2236–2241.

DOI: 10.1021/acscatal.7b03594.

37. S. Liu, Y. Jiang, M. Yang; M. Zhang, Q. Guo, W. Shen, R. He, M. Li, Highly conductive and metallic cobalt-nickel selenide nanorods supported on Ni foam as an efficient electrocatalyst for alkaline water splitting, *NanoScale*, 2019, **11**, 7959–7966. DOI: 10.1039/C8NR10545F.